

## Auroral Hiss Observed by Antarctic Rockets, S-210JA-20 and 21

Iwane KIMURA\*, Toshio MATSUO\*, Tetsuo KAMADA\*\*  
and Isamu NAGANO\*\*\*

南極ロケット S-210JA-20, 21 によるオーロラヒスの観測

木村磐根\*・松尾敏郎\*・鎌田哲夫\*\*・長野 勇\*\*\*

**要旨:** 南極ロケット S-210JA-20, 21 号機で観測されたオーロラヒスについて述べる。前者は地磁気じょう乱時に発射されたが、後者は静穏時であり、ともにオーロラ中に打ち込まれた。

両ロケットで観測されたヒスのスペクトルで電界と磁界の比を求めた結果、このヒスが、ホイスターモード波であることが判明した。

このオーロラヒスのロケットで観測されたポインティング電力と昭和基地上での電力の差は、下部電離層を通過の減衰により定量的に説明がつけられることがわかった。

ロケットで観測された VLF 雑音強度の時間変化が、同じロケットで観測された 40–60 keV の電子および電子密度の変化と比べられたところ、特に 20 号機の 40–60 keV 電子とオーロラヒスの相関はよいが、21 号機はよくないという結果となった。

**Abstract:** Characteristics of auroral hiss emissions observed in the Antarctic rocket experiments using the S-210JA-20 and 21 rockets are described. The S-210JA-20 rocket was launched in a geomagnetically disturbed condition, whereas the S-210JA-21 was launched in a calm condition, although the both penetrated into auroras.

From the ratio of the electric field intensity to the magnetic field intensity, the hiss emissions observed on the above two rockets are identified as the whistler mode.

The Poynting fluxes of the auroral hiss observed on the rockets are compared with those observed on the ground and the difference in the flux is found to be ascribed to the attenuation through the lower ionosphere.

Time variations of the VLF noise intensity observed on the rockets are compared with those of electron flux of 40–60 keV and electron density simultaneously

---

\* 京都大学工学部電気工学第二教室. Department of Electrical Engineering II, Faculty of Engineering, Kyoto University, Yoshida-Honmachi, Sakyo-ku, Kyoto 606.

\*\* 名古屋大学空電研究所. Research Institute of Atmospheric, Nagoya University, 13, Honohara 3-chome, Toyokawa 442.

\*\*\* 金沢大学工学部電気工学科. Department of Electrical Engineering, Kanazawa University, 40–20, Odateno 2-chome, Kanazawa 920.

observed on the same rockets. It is found that the VLF noise level corresponding to the auroral hiss is well correlated with the electron flux in the S-210JA-20 experiment, but the correlation is not good in the S-210JA-21 experiment.

## 1. Introduction

Many rockets have been launched at Syowa Station in the IMS period. One of the main objectives of the experiments is to investigate the interrelation between wave phenomena in auroras and energetic particles. The S-310JA-1 rocket was the first rocket launched in February 1976 for this project, which measured VLF chorus or ELF hiss in a frequency range from 0.2 to 1 kHz (KIMURA *et al.*, 1978). Flux of keV energy electron observed on the same rocket did not show any well defined correlation with the above VLF noise intensity, the fact being understandable, since the chorus or ELF hiss is considered to be generated in a region far away from the rocket altitude (KIMURA *et al.*, 1980).

Two succeeding rockets, S-210JA-20 and 21 were also launched in 1976, one on June 25 and the other on July 26. These rockets were equipped with a VLF wide band receiver, an HF sweep frequency receiver, particle counters using proportional counter and plastic scintillator, and electron density and temperature probes.

The geomagnetic condition in which the rockets were launched was very active for S-210JA-20 and was rather quiet for S-210JA-21, though auroras were present in both experiments.

In the present paper, we pay special attention to auroral hiss observed by these rockets. The mode of propagation will be discussed by investigating the ratio of electric and magnetic field intensities of the observed hiss. The Poynting fluxes of the hiss observed on the rockets are compared with those observed on the ground, and the differences in the flux are ascribed to the attenuation of the wave suffering from the propagation in the lower ionosphere, which can be calculated by the full wave analysis.

The auroral hiss observed on the rockets is also compared with energetic electron flux and electron density simultaneously observed.

## 2. Rocket-Borne Instruments for VLF Observations

Instruments for VLF plasma wave observation (named PWL) on board the S-210JA-20 and 21 rockets were very similar to those installed on S-310JA-1, and the sensors used were a 2.4 m tip-to-tip dipole antenna and a 16000 turn loop antenna wound on a  $1\text{ cm}\phi \times 15\text{ cm}$  long ferrite core.

The block diagram of PWL is shown in Fig. 1. The outputs of preamplifiers of

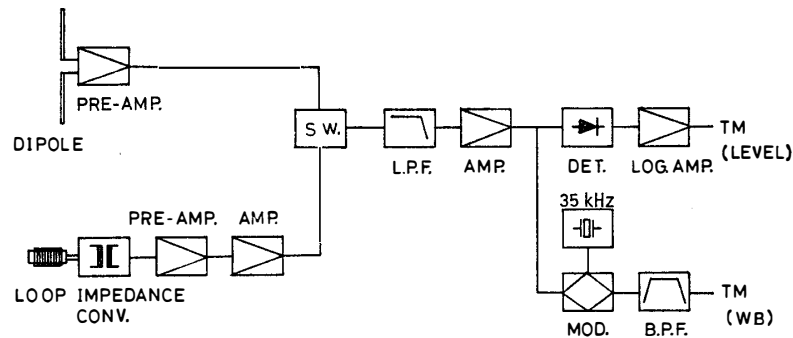


Fig. 1. Block diagram of PWL on board the S-210JA-20 and 21 rockets.

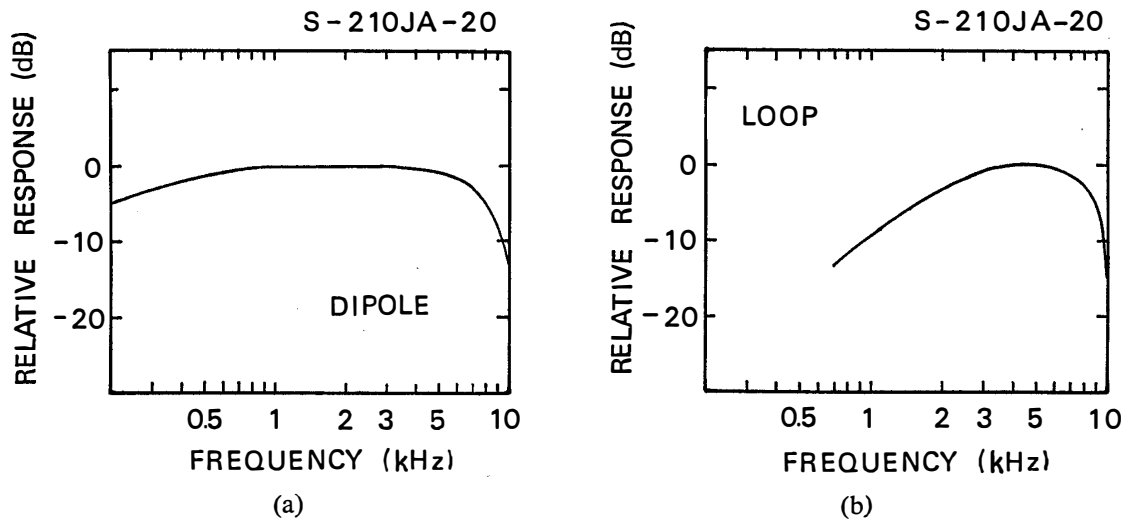


Fig. 2. Frequency characteristics of the dipole (a) and loop (b) antennas including pre-amplifiers on board S-210JA-20.

the dipole and loop antennas are led to the common main amplifier by time sharing with intervals of 10 seconds for *E* and 5 seconds for *B* field. During the first half of the *E* interval, a 3 volt DC bias was applied to the dipole antenna to remove the ion sheath to be produced around the antenna.

The frequency characteristics of the dipole and loop antennas including preamplifiers are shown in Fig. 2 a, b and Fig. 3 a, b for S-210JA-20 and 21 respectively. The effective length of the loop antenna itself in free space was 8.6 mm at 5 kHz for S-210JA-20 and 11 mm at 6 kHz for S-210JA-21.

The VLF wide band data were sent to the ground by a wide band telemetry and the envelope level information was telemetered by IRIG No. 9 channel.

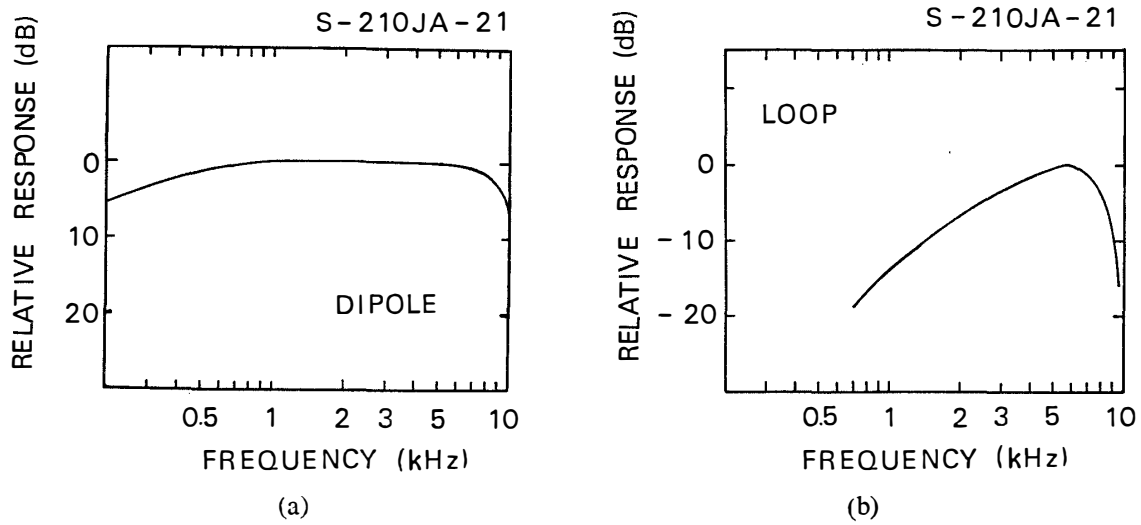


Fig. 3. Frequency characteristics of the dipole (a) and loop (b) antennas including pre-amplifiers on board S-210JA-21.

### 3. Ground and Satellite Observations at the Time of the Rocket Launching

#### 3.1. S-210JA-20

The rocket was launched into a diffuse aurora at 02:40:30 LT on June 25, 1976, and reached an altitude of 118 km, when it was in the midst of  $-400 \gamma$  substorm (see Fig. 4). Cosmic absorption (CNA) was  $-0.8$  dB. Ground based VLF hiss recorder data at 8 and 64 kHz are shown in comparison with 5577 and 6300 Å intensity in Fig.

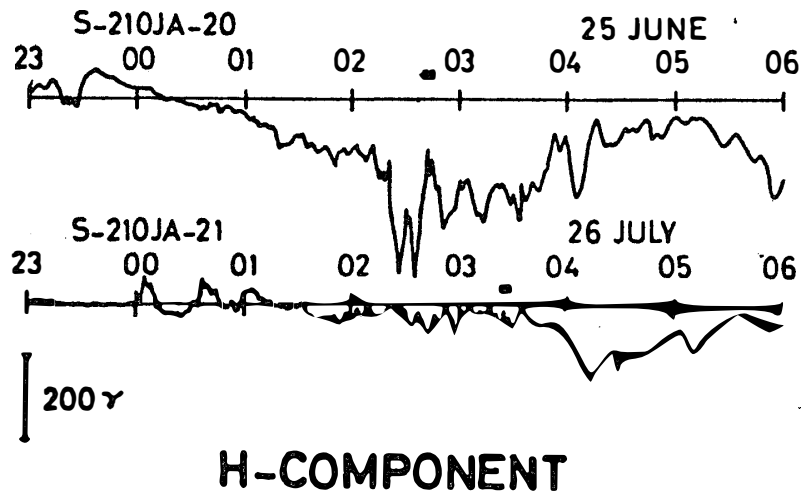


Fig. 4. Geomagnetic variation at the time of rocket launching.

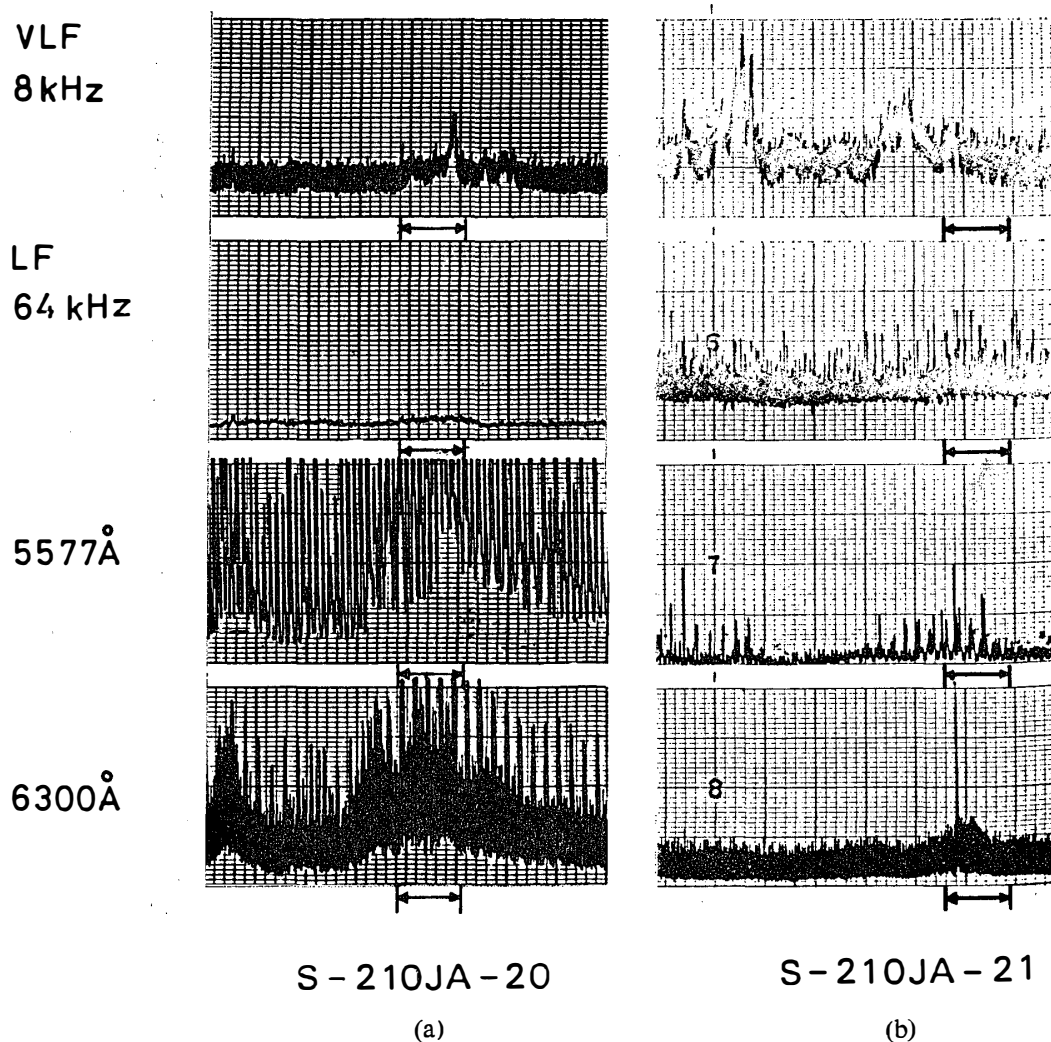


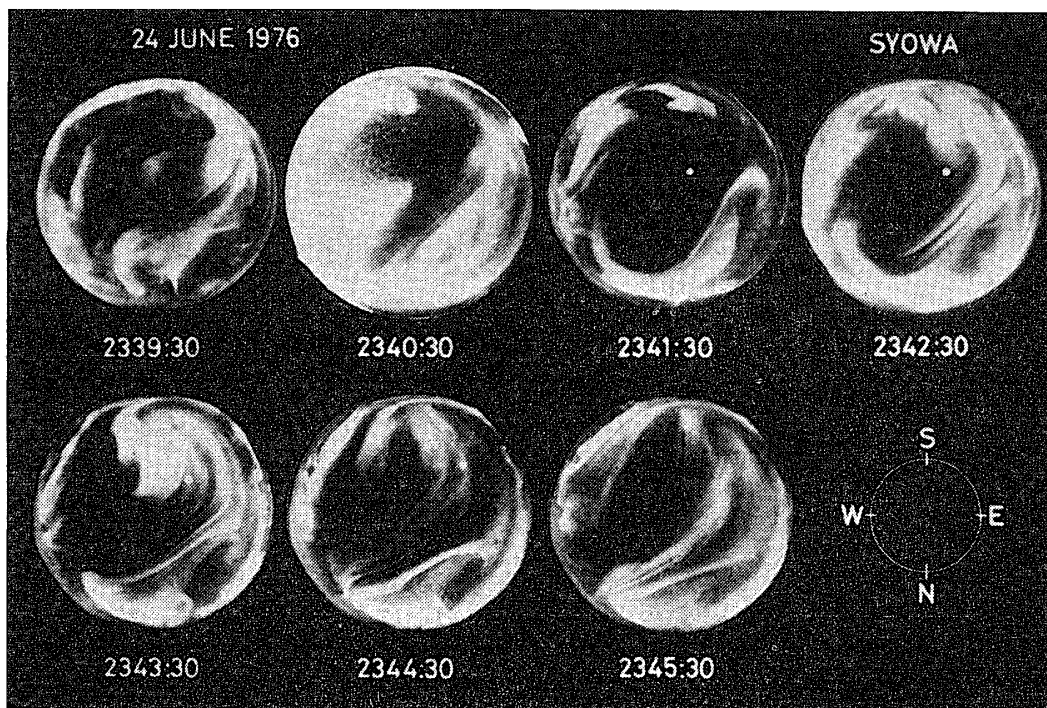
Fig. 5. Hiss intensity at 8 and 64 kHz and auroral luminosity at 5577 and 6300 Å observed at Syowa Station at the time of S-210JA-20 (a) and 21 (b) rocket launching.

5a and all sky camera data are shown in Fig. 6a, VLF power flux densities at 0.75, 1, 2 and 8 kHz observed on the ground are shown in Fig. 7a. There is an enhancement of hiss at 8 kHz correlated with enhancement of auroral luminosity.

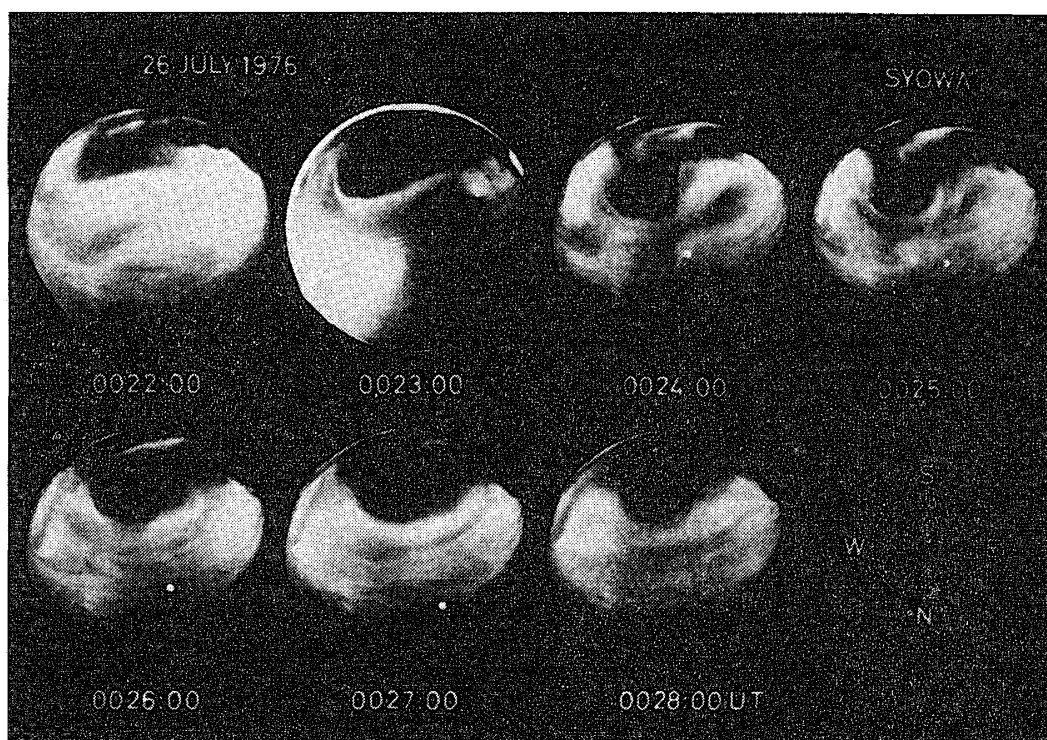
The VLF wide band spectrum observed on the ground is shown in Fig. 8. ISIS-2 satellite passed in a distance of 1200 km east of Syowa Station, observed VLF spectrum as shown in Fig. 9. From these spectra, it is concluded that VLF hiss was present on the ground and at the satellite altitude ( $\sim 1450$  km).

### 3.2. S-210JA-21

This rocket was launched also into an aurora at 03:23:00 LT on July 26, 1976



(a)



(b)

Fig. 6. Aurora luminosity observed by all sky camera at Syowa Station at the time of S-210JA-20 (a) and 21 (b) rocket launching. White dots in the picture indicate the location of the rocket.

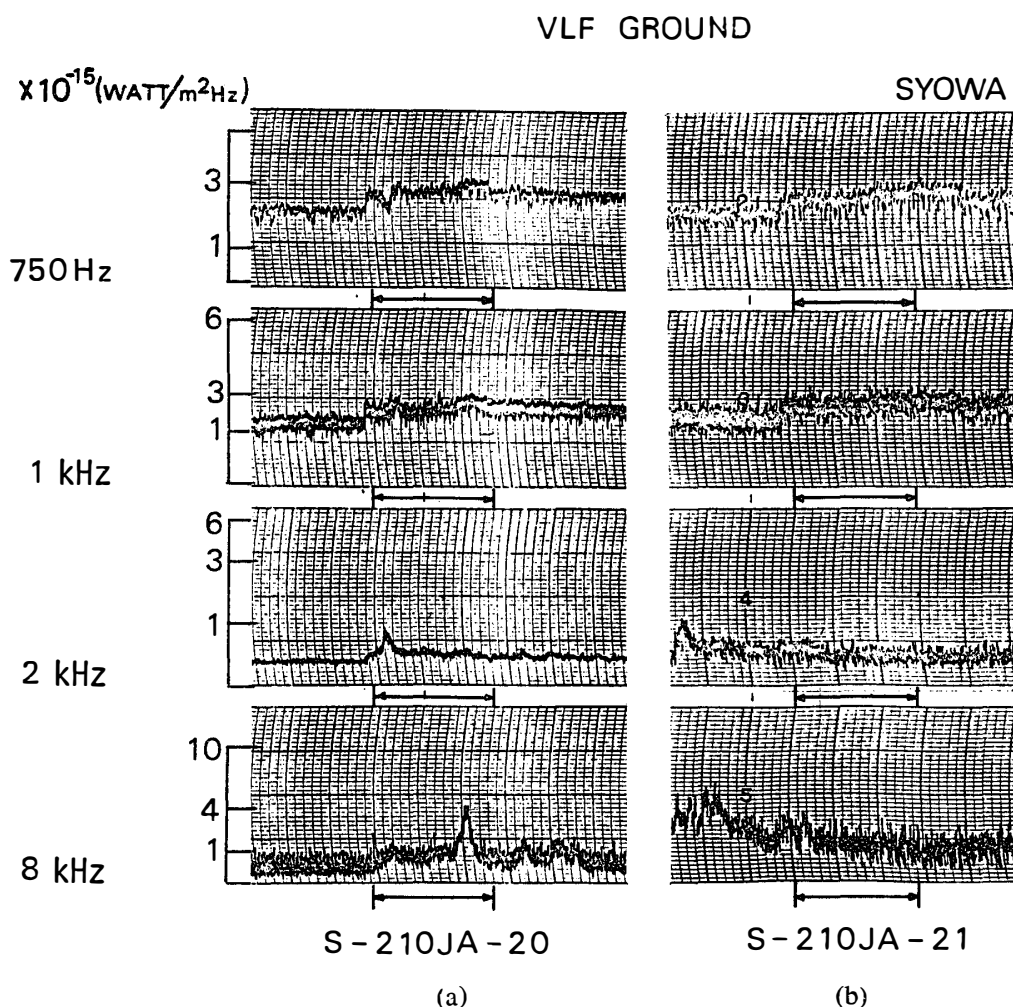
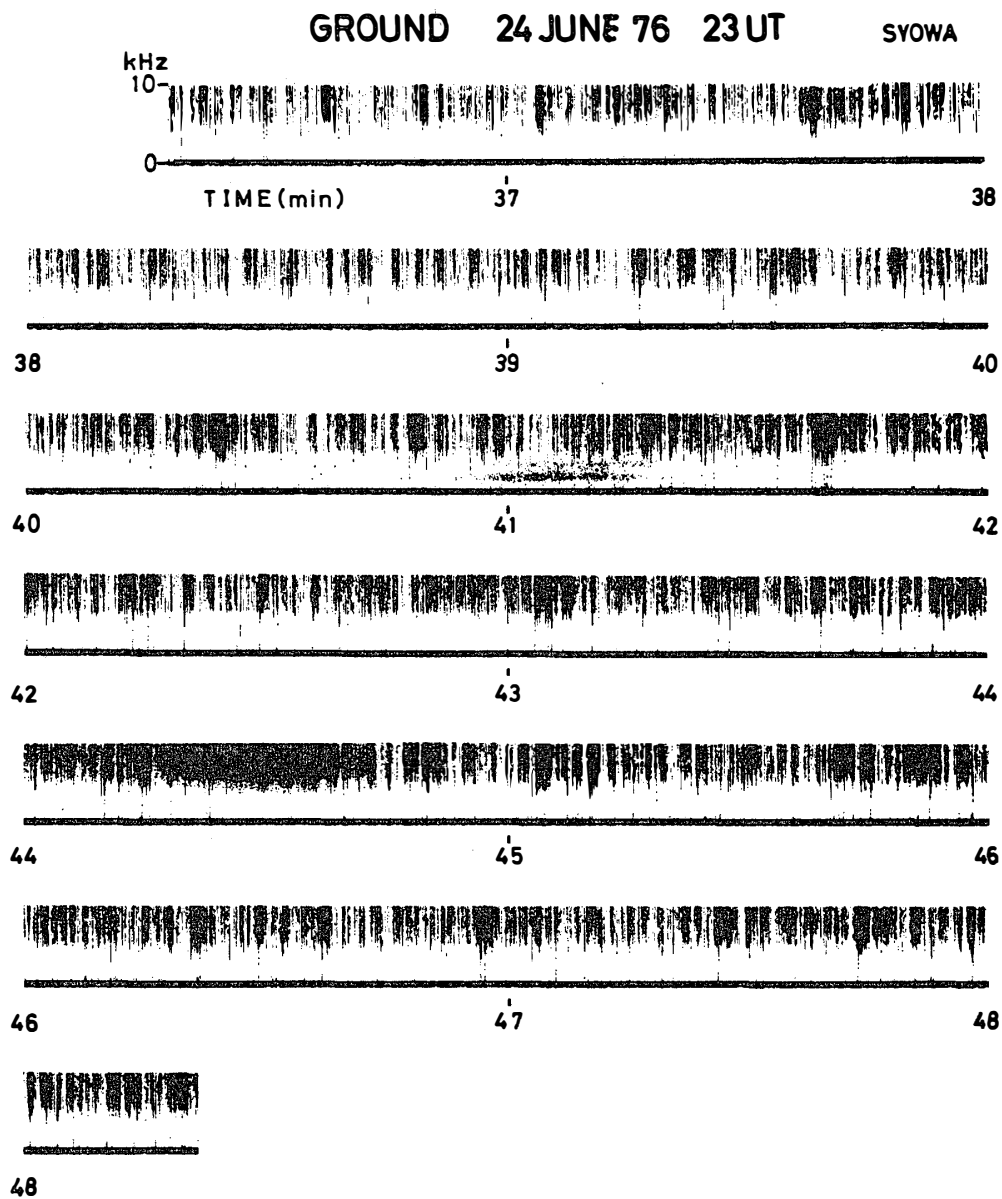


Fig. 7. VLF power flux densities at 0.75, 1, 2, and 8 kHz observed at Syowa Station at the time of S-210JA-20 (a) and 21 (b) rocket launching.

and reached an altitude of 116 km, when it was geomagnetically quiet. The intensity of CNA was  $-0.1$  dB. Auroral luminosity at  $5577 \text{ \AA}$ , and  $6300 \text{ \AA}$ , all sky camera photographs and VLF intensity observed on the ground are shown in Figs. 5b, 6b, and 7b.

The VLF wide band spectrum on the ground is shown in Fig. 10. The satellite ISIS-1 passed over Syowa Station 03:25 LT and the VLF spectrum observed is shown in Fig. 11. It is clear that hiss was present at the satellite position, although the data are contaminated by interference of other instruments. On the ground, although the spectrum in Fig. 10 is covered by strong atmospheric, it is evident from Fig. 7b and Fig. 10 that hiss was present at least several minutes before the rocket launching.



*Fig. 8. VLF wide band spectrum observed at Syowa Station at the time of S-210JA-20 rocket launching.*

#### 4. Rocket Observation of Auroral Hiss

Dynamic frequency spectra of the wide band signals are shown in Figs. 12 and 13 for S-210JA-20 and 21 respectively. The detailed frequency spectra at sampled altitudes in the ascending and descending time of S-210JA-20 are shown in Figs. 14 a and b and those of S-210JA-21 are shown in Figs. 15 a and b.

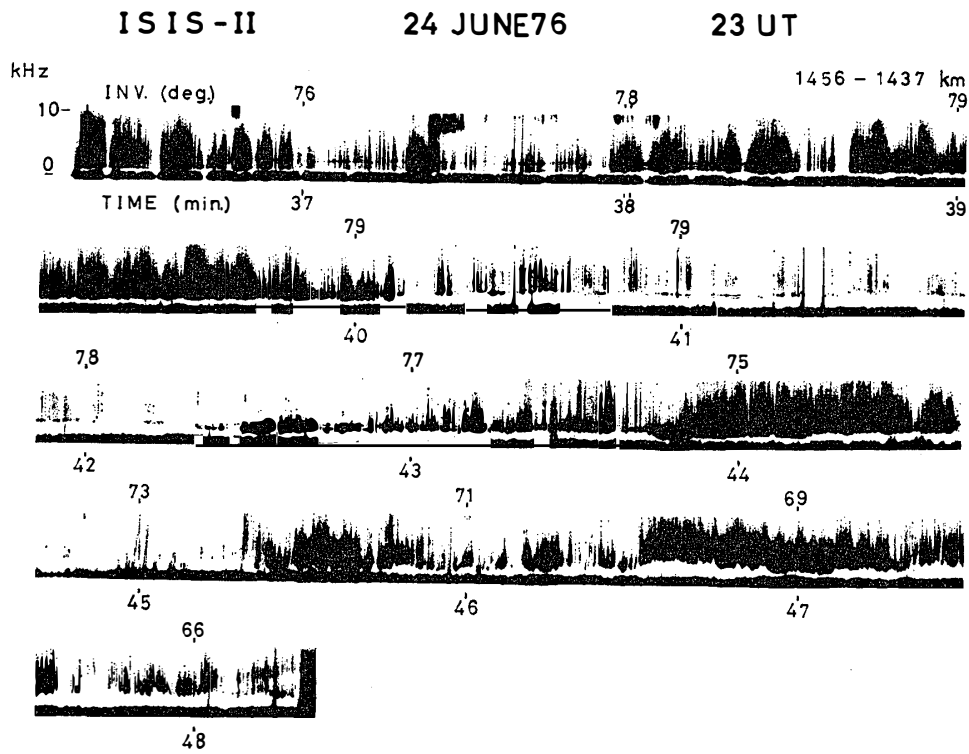


Fig. 9. VLF wide band spectrum observed on the ISIS-2 satellite.

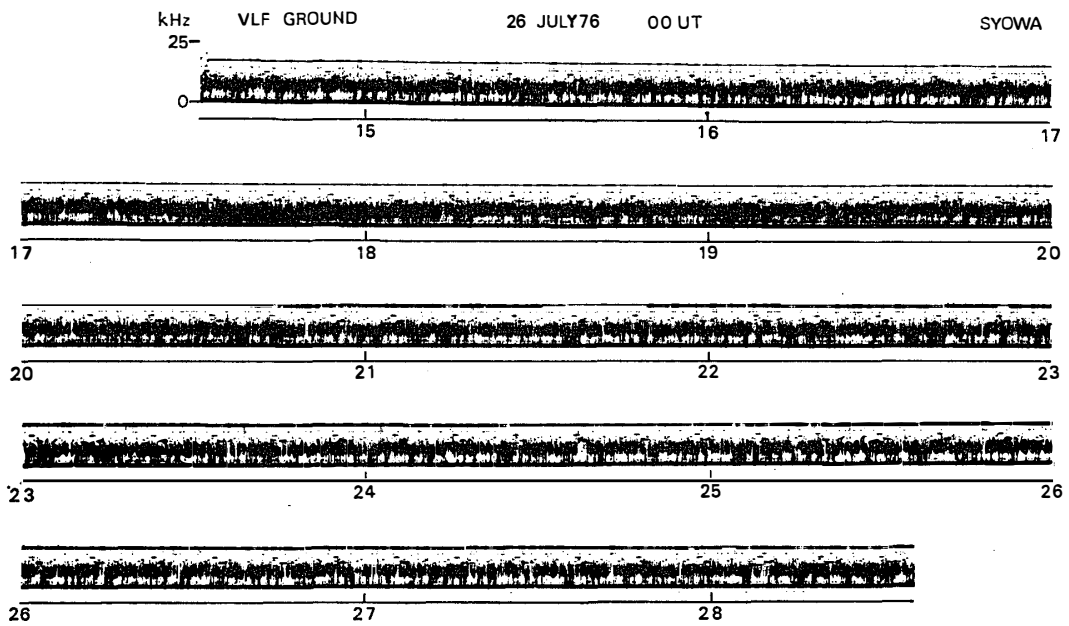


Fig. 10. VLF wide band spectrum observed at Syowa Station at the time of S-210JA-21 rocket launching.

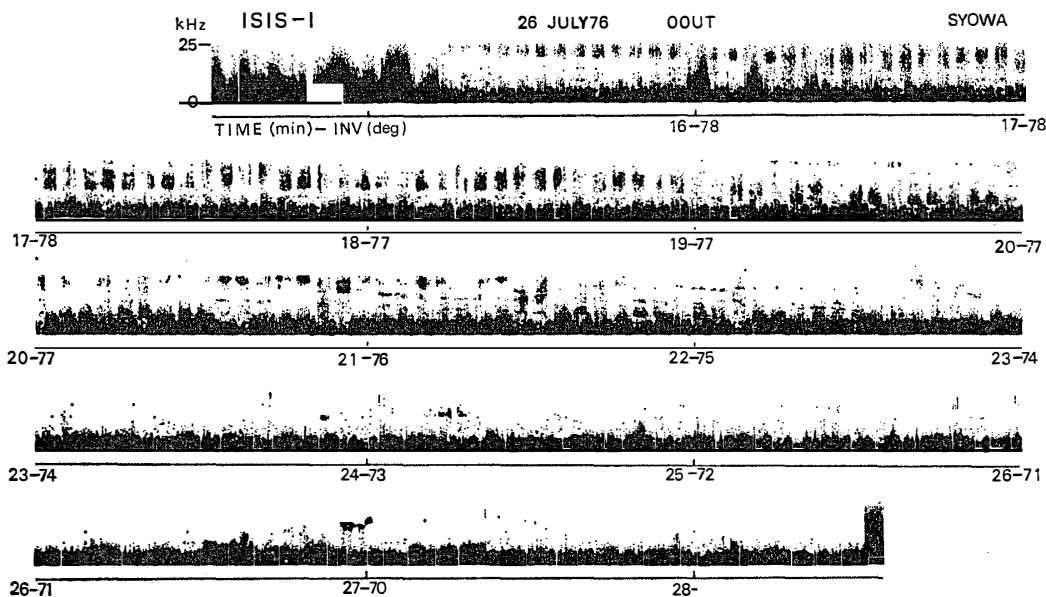


Fig. 11. VLF wide band spectrum observed on the ISIS-1 satellite.

#### 4.1. Mode of propagation

From these spectra, we can make altitude profiles of the intensity of dipole and loop antenna outputs, when we pay attention to a particular frequency band, say 6–7 kHz or 7–8 kHz. Fig. 16a (left) illustrates the altitude profiles of the dipole and loop signal intensities in a 7–8 kHz band in the S-210JA-20 experiment. The notation D(3) implies that the dipole outputs were sampled for the interval when the 3 volt DC bias was on to the dipole antenna. The ratios of D(3) intensity to L intensity which are equal to the differences between the D(3) and L intensities in dB are shown in the Fig. 16 b.

If the signals are in the whistler mode, the above ratio must agree with those calculated by taking into account 1) the difference in effective length of the dipole and the loop antennas, 2) the difference in gain of the dipole and the loop antenna channels and 3) the refractive index and the wave normal angle to the geomagnetic field. The ratio was calculated by assuming that the wave normal angle is simply zero (*cf.* Fig. 16 b). From this figure, it is evident that the calculated lines show rather good agreement with those obtained from the observed data, within a 5 dB difference, implying that the signals analyzed are the whistler mode.

In the same way, the observed and calculated lines are drawn for S-210JA-21 in Figs. 17 a and b. In this case, the agreement is also satisfactory at the altitudes higher than 100 km.

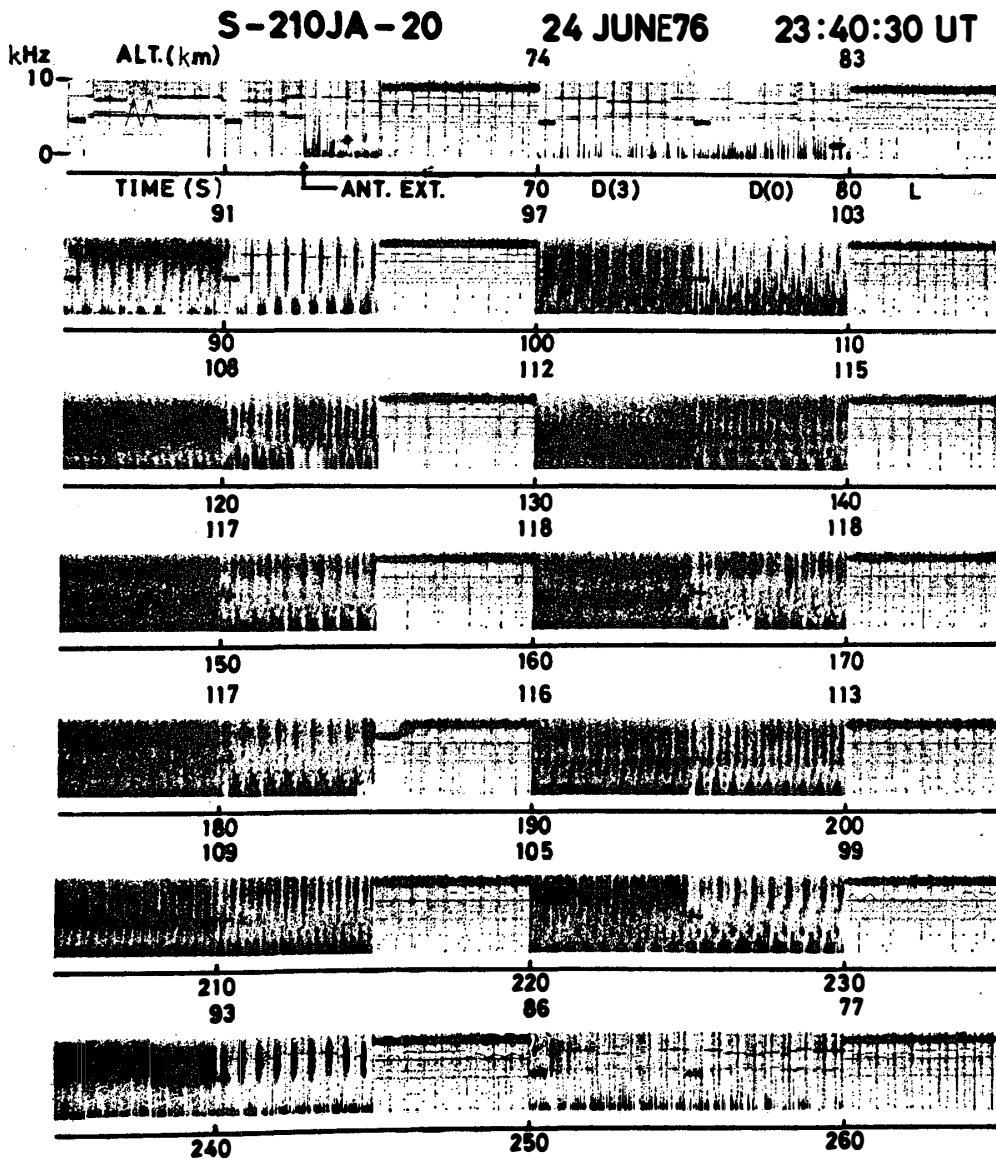


Fig. 12. VLF wide band spectrum observed on S-210JA-20.

**4.2. Poynting flux and absorption through the lower ionosphere**

From the field intensities of auroral hiss observed by the rockets, the Poynting fluxes are determined, which are also compared with those observed on the ground. Comparisons at some sampled altitudes of the rockets are shown in Table 1. Absorptions through the lower ionosphere, deduced from the difference in Poynting flux between those observed on the rocket and on the ground, are also shown in the table.

On the other hand, we can calculate the attenuation of the VLF waves through

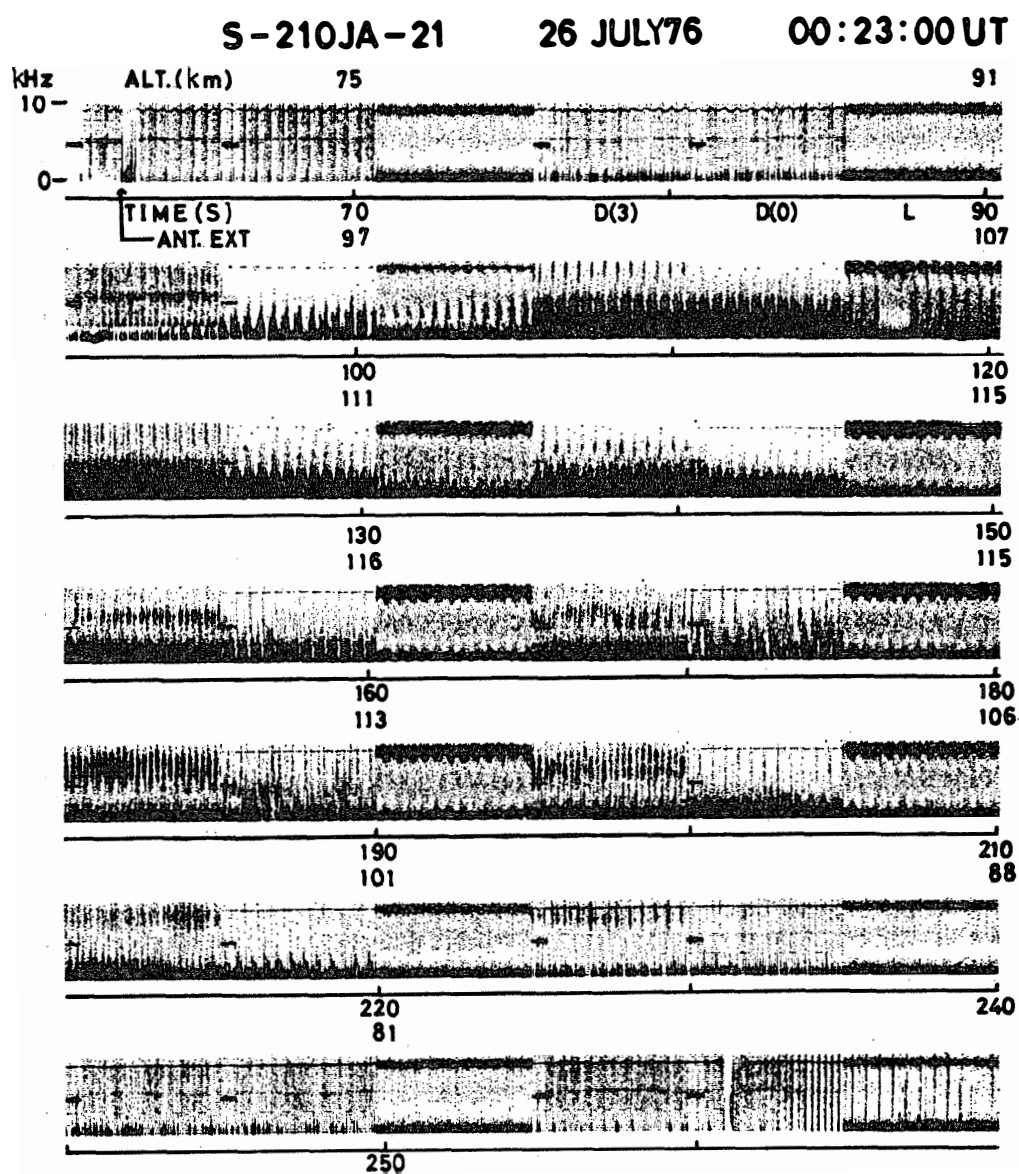


Fig. 13. VLF wide band spectrum observed on S-210JA-21.

Table 1. Comparisons of auroral hiss intensity observed by S-210JA-20 and S-210JA-21.

	S-210JA-20	S-210JA-21
Altitude	96 km	115 km
Frequency	7-8 kHz	6-7 kHz
Electric field	7.5 $\mu\text{V/m}$	5.1 $\mu\text{V/m}$
Refractive index	18	37
Poynting flux (rocket)	$6 \times 10^{-14} \text{W/m}^2\text{Hz}$	$5.6 \times 10^{-14} \text{W/m}^2\text{Hz}$
Poynting flux (ground)	$\sim 1.5 \times 10^{-15}$	$\sim 2.5 \times 10^{-15}$
Attenuation	$\sim 16 \text{ dB}$	$\sim 14 \text{ dB}$

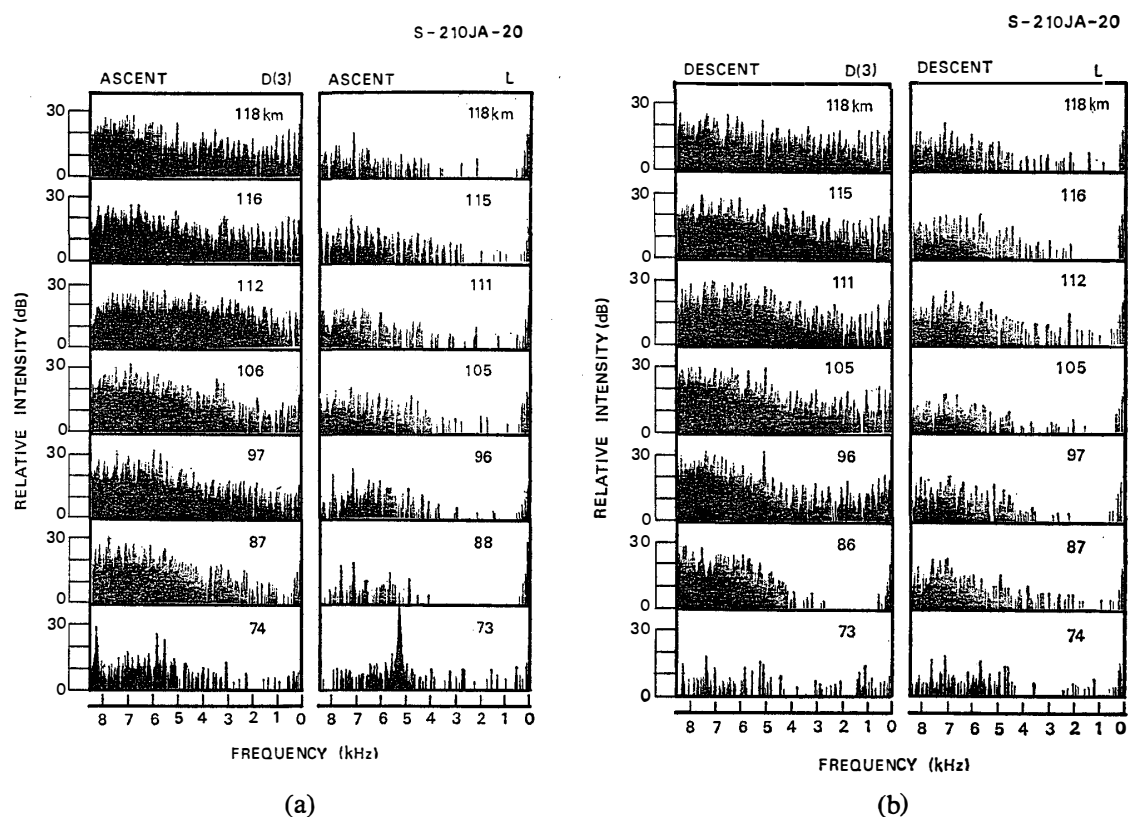


Fig. 14. Frequency spectra at sampled altitudes in the ascending (a) and descending flight time (b) of S-210JA-20.

the lower ionosphere, since we have electron density profiles simultaneously observed on the rockets. A dependence of the attenuation in Poynting flux upon the incident wave normal angle is shown in Fig. 18. The attenuation was calculated by a computer program for the full wave analysis developed by NAGANO *et al.* (1975), using the electron density profile as shown in Fig. 19, which was actually observed in the ascending time of S-210JA-20, the collision frequency profile as shown in Fig. 20, and the geomagnetic dip angle at Syowa Station. From this figure, it is evident that the attenuation becomes minimum for the wave normal angle  $1^\circ$  toward the north from the vertical, the minimum being  $-14$  dB. This quantity is satisfactorily consistent with the observed value ( $-16$  dB).

#### 4.3. Correlation of VLF noise intensity with energetic electrons simultaneously observed on the same rockets

The VLF noise intensity indicated by the level output in the block diagram of Fig. 1 was sampled and is drawn with time and altitudes as in Fig. 21a in which the maximum and minimum intensities of the spin modulated amplitudes are separately drawn. This

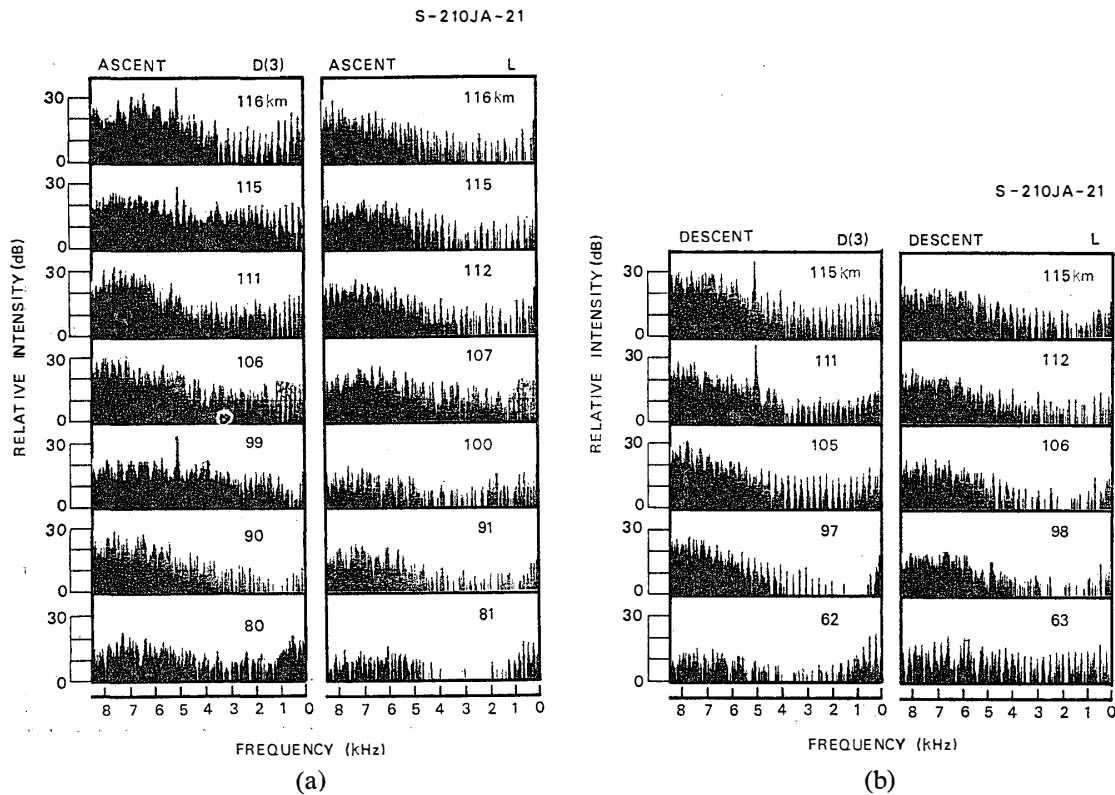


Fig. 15. Frequency spectra at sampled altitudes in the ascending (a) and descending flight time (b) of S-210JA-21.

figure shows the result of the S-210JA-20 rocket measurement. Fig. 21b shows the flux of 40–60 keV electrons at a pitch angle of  $105^\circ$  (KODAMA *et al.*, 1980) and the electron density (MIYAZAKI *et al.*, 1980), simultaneously measured on the same rocket. From Fig. 21a, b, c, it is evident that the minimum level of the VLF noise intensity shows a good correlation with the 40–60 keV electron flux. The flux of electrons with energy higher than 60 keV did not show such a good correlation as the flux in the 40–60 keV range. The peak level in Fig. 21a seems to indicate the intensity of electrostatic noises, whereas the minimum level seems to represent the auroral hiss intensity. Thus it is concluded that there is a good correlation between the energetic electrons of 40–60 keV and the auroral hiss intensity in the S-210JA-20 experiment.

The result of the S-210JA-21 is given in Fig. 22 in which the notation is same as that in Fig. 21. The correlation between the VLF noise level and the energetic electron flux is not always sufficiently good, as compared with the S-210JA-20 case.

As to the relationship of the VLF noise intensity with the electron density, it is evident that the VLF noise intensity suddenly decreases below the ionosphere. This

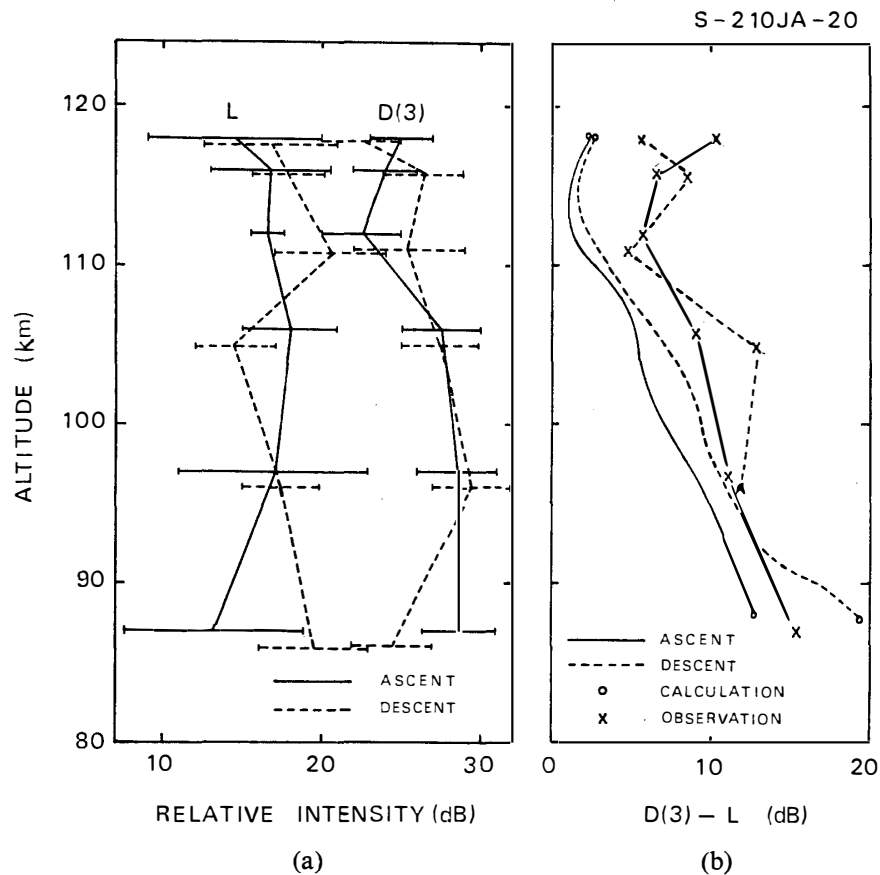


Fig. 16. (a) Altitude profile of the noise intensity in a 7-8 kHz band observed by S-210JA-20.  $D(3)$  stands for the output of dipole antenna with DC bias and  $L$  stands for the output of loop antenna. (b) Ratio of the intensity of  $D(3)$  to that of  $L$ , which is equivalent to the difference of  $D(3)$  and  $L$  in dB.

attenuation is due to the collisional absorption of VLF waves through the lower ionosphere.

## 5. Conclusion

VLF wave phenomena observed by S-210JA-20 and 21 were investigated in detail. Although electrostatic wave phenomena were also involved in the spectra, the spectral component higher than 6 kHz was identified as auroral hiss in the whistler mode.

The Poynting flux observed on the ground was about 16 dB-14 dB smaller than those observed in the ionosphere by the rockets. A full wave calculation of a VLF

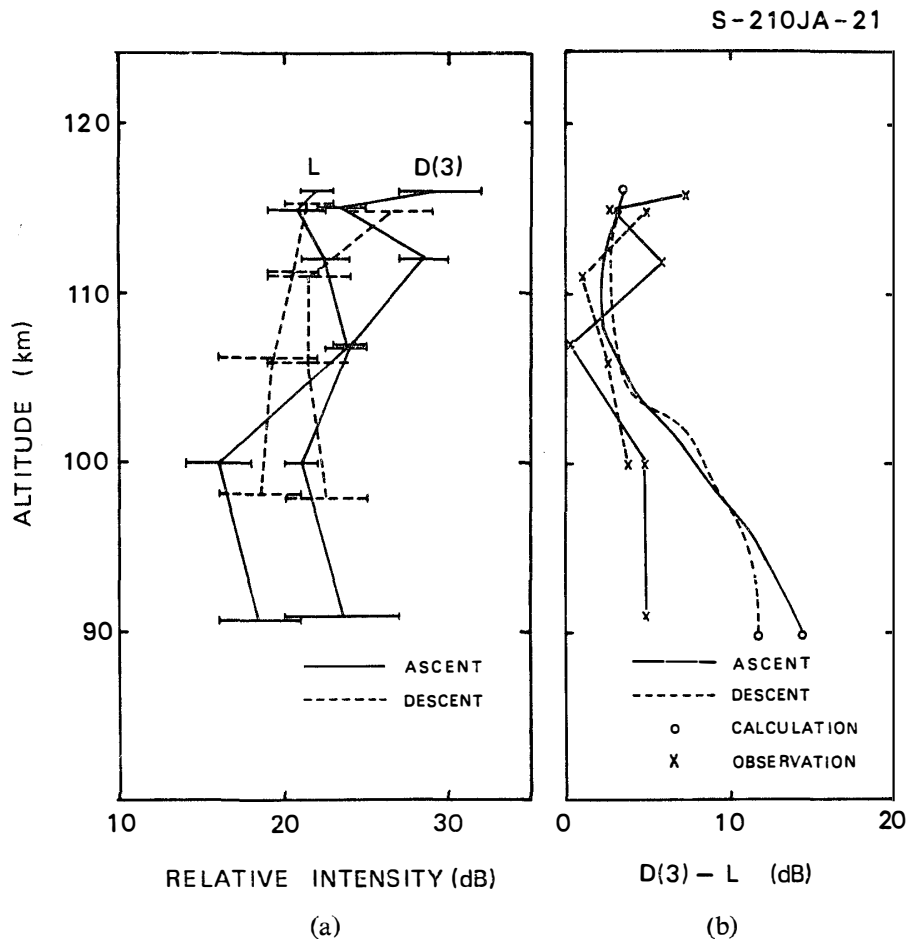


Fig. 17. (a) Altitude profile of the noise intensity for a 6-7 kHz band observed by S-210JA-21.  $D(3)$  represents the output of dipole antenna with DC bias and  $L$  represents the output of loop antenna. (b) Ratio of the intensity of  $D(3)$  to that of  $L$ , which is equivalent to the difference between  $D(3)$  and  $L$  in dB.

wave propagating downward through the lower ionosphere gives the wave attenuation of 16 dB for the electron density profile observed by S-210JA-20. The calculated intensity of attenuation shows a good agreement with the observed value.

As to the relationship of auroral hiss with energetic electrons, a qualitatively good correlation was found in the S-210JA-20 rocket experiment, whereas no clear relationship was found in the S-210JA-21 case. Where is the source of auroral hiss located? This has been an interesting question to the auroral hiss. In the ground observation, auroral hiss has sometime indicated a close correlation with auroral luminosity. This fact may be an evidence that the hiss is generated in the ionosphere directly by the electrons responsible to the aurora.

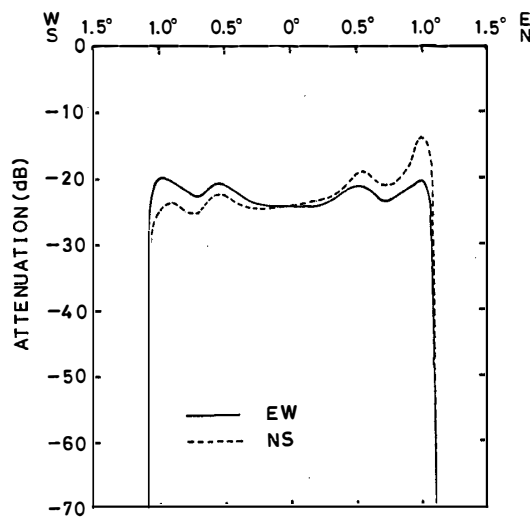


Fig. 18. Dependence of the attenuation in Poynting flux upon the incident wave normal angle measured from the vertically downward direction.

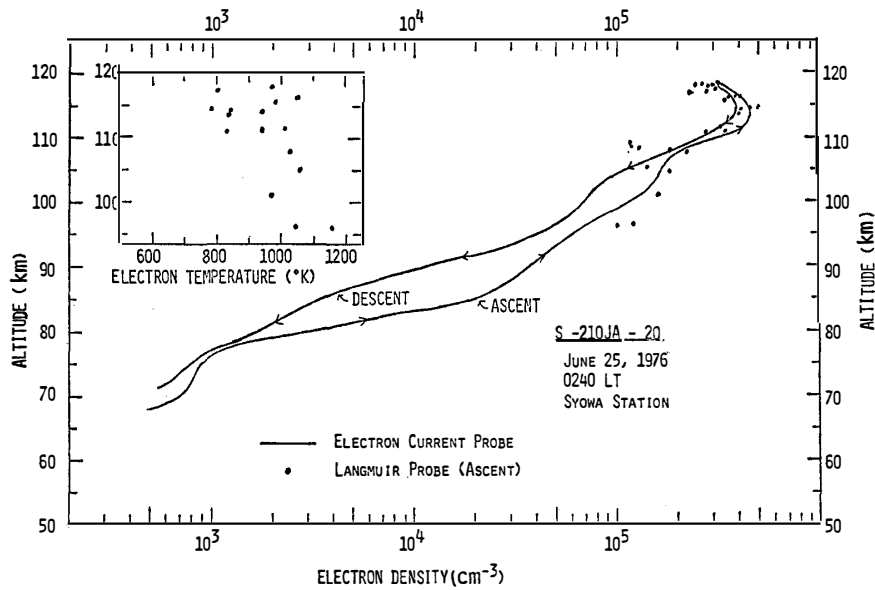


Fig. 19. The electron density profile simultaneously observed on S-210JA-20. The ascent profile is used for the full wave calculation.

Our rocket experiments indicate that the S-210JA-20 case may support the above mechanism, but the other case does not. Therefore, it is concluded that the generation mechanism is not so simple. Further rocket experiments are needed in the future.

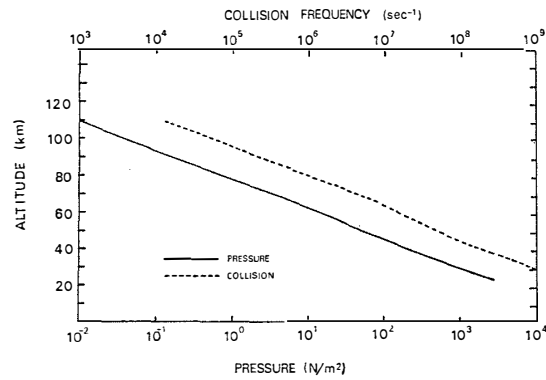


Fig. 20. Collision frequency profile which is used for the full wave calculation.

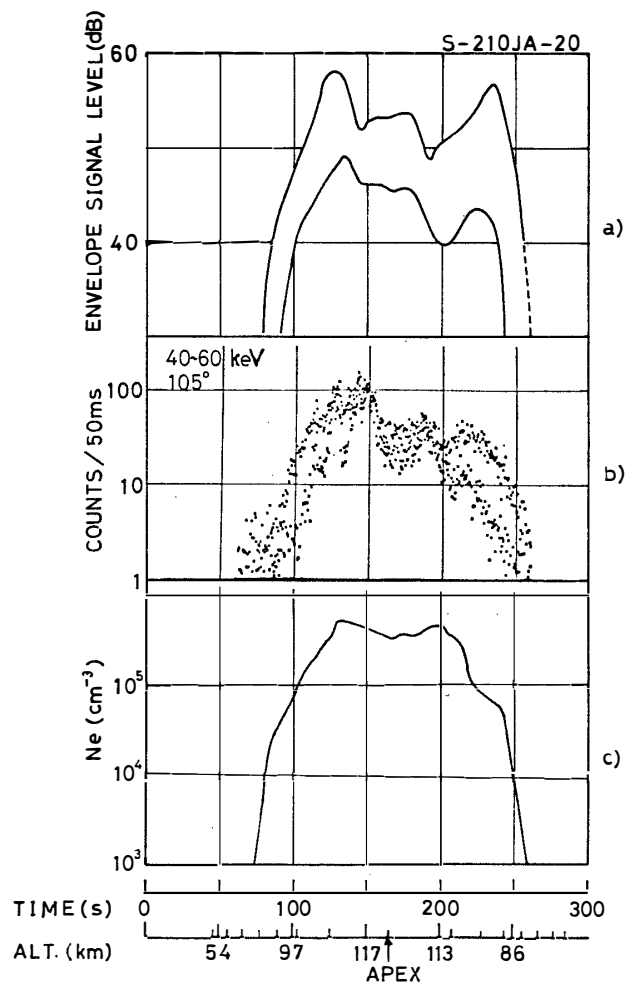


Fig. 21. Time variations of VLF noise intensity (a), energetic electron flux (b) and electron density (c) observed by S-210JA-20.

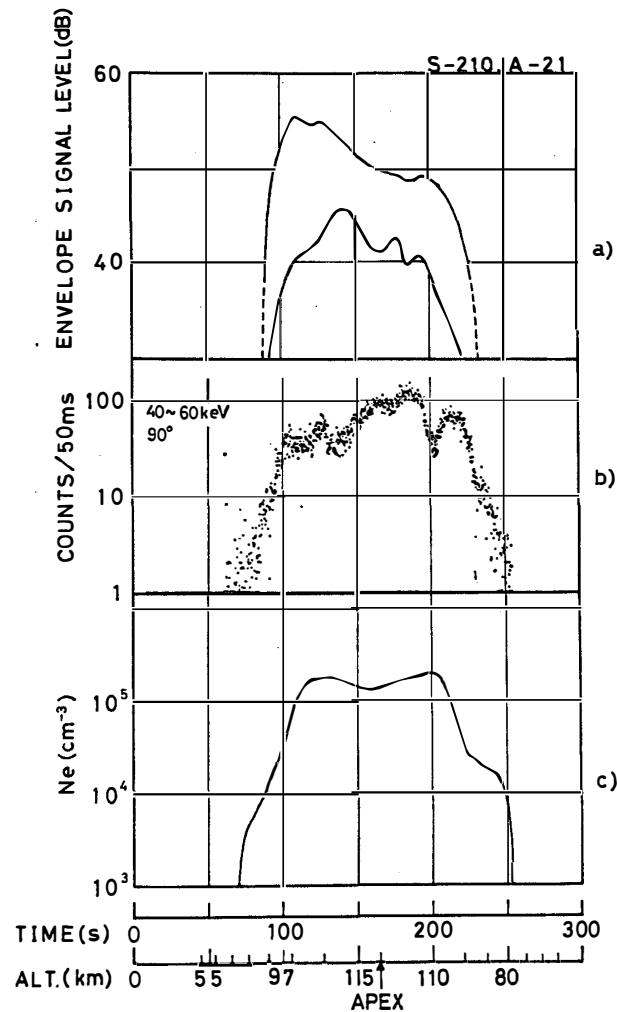


Fig. 22. Time variations of VLF noise intensity (a), energetic electron flux (b) and electron density (c) observed by S-210JA-21.

#### Acknowledgments

We wish to express our thanks to the members of the 17th wintering party of Japanese Antarctic Research Expedition, headed by Prof. T. YOSHINO, for their effort in launching the rockets in severe conditions and in making the ground-based observations. We are also grateful to Dr. M. KODAMA and other staff members of the Institute of Physical and Chemical Research and Dr. S. MIYAZAKI and other staff members of Radio Research Laboratories, who provided us with the data of energetic electrons and electron density observed by the same rockets.

#### References

KIMURA, I., YAMAGISHI, H., MATSUO, T. and KAMADA, T. (1978): S-310JA-1 rocket observation of

- VLF emission spectra at Syowa Station in Antarctica. Mem. Natl Inst. Polar Res., Spec. Issue, **9**, 51–68.
- KIMURA, I., MATSUO, T., YAMAGISHI, H., KAMADA, T. and TSURUDA, K. (1980): S-310JA-1, 2 gôki ni yoru VLF shizen denjiha-purazuma-ha no sokutei (VLF natural radio and plasma wave observations by S-310JA-1 and 2 rockets). Nankyoku Shiryô (Antarct. Rec.), **69**, 63–70.
- KODAMA, K., OKUTANI, S., WADA, M., IMAI, T. and TAKEUCHI, H. (1980): Roketto kôdo ni okeru >40 keV ôrora denshi no picchi kaku bunpu (Pitch angle distribution of >40 keV auroral electrons observed at rocket altitudes). Nankyoku Shiryô (Antarct. Rec.), **68**, 35–46.
- MIYAZAKI, A., MORI, H. and OGAWA, T. (1980): S-210JA-20, 21 gôki ni yoru denshi mitsudo ondo kansoku kekka (Observational results of electron density and temperature in the polar ionosphere by S-210JA-20 and 21 rockets). Nankyoku Shiryô (Antarct. Rec.), **69**, 52–55.
- NAGANO, I., MAMBO, M. and FUTATSUISHI, G. (1975): Numerical calculation of electromagnetic waves in an anisotropic multi-layered medium. Radio Sci., **10**, 611–617.

(Received May 17, 1979)